Passive wireless frequency doubling antenna sensor for strain and crack sensing

Chunhee Cho, Xiaohua Yi, Dan Li, Yang Wang, Member, *IEEE*, Manos M. Tentzeris, Fellow, *IEEE*

***Abstract*—This research presents the design, simulation, and validation experiments of a passive (battery-free) wireless frequency doubling antenna sensor for strain and crack sensing. Since the length of a patch antenna governs the antenna's resonance frequency, a patch antenna bonded to a structural surface can be used to measure mechanical strain or crack propagation by interrogating resonance frequency shift due to antenna length change. In comparison with previous approaches such as radio frequency identification, the frequency doubling scheme is proposed as a new signal modulation approach for the antenna sensor. The proposed approach can easily distinguish backscattered passive sensor signal (at the doubled frequency $2f$) from environmental electromagnetic reflections (at original reader interrogation frequency f). To accurately estimate the performance of the frequency doubling antenna sensor, a multi-physics coupled simulation framework is proposed to aid the sensor design while considering both the mechanical and electromagnetic behaviors. Two commercial software packages, COMSOL and ADS, are combined to leverage the features from each other. The simulated performance of the frequency doubling antenna sensor is further validated by experiments. The results show that the sensor is capable of detecting small strain changes and the growth of a small crack.**

***Index Terms*— Crack sensing, frequency doubling, patch antenna, strain sensing.**

I. Introduction

In order to accurately assess deterioration of civil, mechanical, and aerospace structures, a large volume of research in structural health monitoring (SHM) has been inspired over the past few decades. SHM systems can advance time-based maintenance into more cost effective condition-based maintenance. Sensors have been developed to measure various structural responses and operating conditions, including strain, displacement, acceleration, humidity, temperature, *etc*. Among the measurements, strain can be an important indicator for stress concentration and crack development. Metal foil strain gages are currently among the most common solutions for strain measurement, owing to their low-cost, simple circuitry, and acceptable reliability in many applications. However, when applied to large structures, either metal foil strain gages or fiber optic strain sensors require lengthy cable connections for power supply and data acquisition, which can significantly increase installation time and system cost [2].

Over the past two decades, cost-effective wireless sensors have been developed to reduce system cost [3-5]. An exhaustive review on wireless sensing for SHM can be found in Lynch and Loh [6], which summarizes development of various academic and industrial wireless sensing devices. A wireless sensing device usually has three functional modules: sensing interface (converting analog sensor signal to digital data), computing core (data storage and processing), and wireless transceiver (digital communication with peers or a wireless gateway server). To obtain different types of measurements, various sensors can be connected with the sensing interface of a wireless sensing device. For example, strain measurement is obtained by interfacing the device with a metal foil strain gage. In addition, most wireless sensing devices usually operate on external power source, such as batteries. To avoid periodic battery replacement in the field, rechargeable batteries are often deployed. These batteries are charged by an integrated energy harvester. Typical sources for energy harvesting include solar energy, mechanical vibration, and thermal gradients, *etc* [7]. However, even with a reliable source for energy harvesting, rechargeable batteries usually have a limited life span. Therefore, passive (battery-free) wireless sensors have been proposed to eliminate the dependency on battery power [8].

Passive wireless strain sensors based on inductive coupling with two adjacent inductors have been developed [9-11]. The interrogation distance achieved by inductive coupling is usually limited to several inches, which is inconvenient for practical applications. Similarly, Matsuzaki *et al* [12] proposed a half wave-length dipole antenna to detect damage in carbon fiber reinforced polymer structures. The damage causes antenna property changes, including power spectrum and return loss, which are measured and used as the damage indicator. Later on, a circular patch antenna sensor was proposed for omnidirectional strain sensing by wirelessly measuring

This material is based upon work supported by the Federal Highway Administration (DTFH61-10-H-00004), the Air Force Office of Scientific Research (FA9550-14-1-0054), and the National Science Foundation (ECCS 1307762. Any opinions, findings, and conclusions or recommendations expressed in this publication are those of the authors and do not necessarily reflect the view of the Federal Highway Administration.

Chunhee Cho is with School of Civil and Environmental Engineering, Georgia Institute of Technology, Atlanta, GA 30332 USA. (e-mail: ccho37@gatech.edu).

Xiaohua Yi was with School of Civil and Environmental Engineering, Georgia Institute of Technology (current address: ExxonMobil Upstream Research Company at Houston, TX 77389; e-mail: yixhzju@gmail.com).

Dan Li is with School of Civil and Environmental Engineering, Georgia Institute of Technology, Atlanta, GA 30332 USA. (e-mail: dli323@gatech.edu).

Yang Wang is with School of Civil and Environmental Engineering, Georgia Institute of Technology, Atlanta, GA 30332 USA. (e-mail: yang.wang@ce.gatech.edu).

Manos M. Tentzeris is with School of Electrical and Computer Engineering, Georgia Institute of Technology, Atlanta, GA 30332 USA (e-mail: etentze@ece.gatech.edu).

scattering parameter [13]. Another passive on-chip radio frequency microelectromechanical system (RF-MEMS) strain sensor is developed for bio-medical application [14]. Without proper signal modulation, the sensor operates in the near field of a reader antenna. As a result, the wirelessly received sensor signal is mixed with background reflection and only limited interrogation distance is achieved.

In order to increase interrogation distance, electromagnetic backscattering techniques have been exploited for wireless strain sensing. For example, a patch antenna has been designed for wireless strain sensing [15, 16], where a phototransistor is adopted for modulating the RF signal backscattered from the antenna sensor. As a result of the modulation, backscattered sensor signal can be distinguished from environmental reflections. However, besides requiring line of sight, the light-switching mechanism is not practical for outdoor application, where light intensity is usually so strong that the phototransistor is constantly activated and thus, loses ability of switching. As another example, passive (battery-free) RFID (radio frequency identification) antennas have been proposed for wireless strain measurement [17, 18]. Through signal modulation by an economic RFID chip (costing about $0.10), patch antennas demonstrate promising performance for wireless strain/crack sensing. However, the current commercial off-the-shelf RFID chips have limited operating frequency range such as 860-960MHz [19]. Because the operating resonance frequency (MHz) approximately equals the strain sensitivity (Hz/με) of an antenna sensor, the RFID antenna sensors have relatively low strain sensitivities. In addition, the antenna resonance frequency is inversely proportional to the length of electrical path, which is relevant to sensor size. The dependency on 900MHz frequency band also dictates that size reduction can be difficult for RFID antenna sensors.

In this paper, a frequency doubling technique is introduced as an alternative way of signal modulation in order to improve strain sensitivity and reduce sensor size while removing unwanted environmental reflections by doubling the backscattered signal frequency. The frequency doubling antenna sensor consists of three main components — a 2.9GHz receiving patch antenna, a matching network, and a 5.8GHz transmitting patch antenna. For interrogation, a wireless reader emits a 2.9GHz interrogation signal to the 2.9GHz receiving patch antenna of the antenna sensor. The matching network integrated with a Schottky diode then doubles the interrogation frequency of 2.9GHz to the backscattering frequency of 5.8GHz. The 5.8GHz transmitting patch antenna finally responds with the backscattered signal to the reader.

A linear scaling model, which simply scales the antenna sensor dimensions according to the applied strain and Poisson's ratio, is commonly used in the previous research [17, 18]. However, this modeling technique does not guarantee the simulated performance of the antenna sensor due to limits of describing mechanical behavior. In this paper, the performance of the frequency doubling antenna sensor is characterized using a commercial software package, COMSOL, which supports mechanical-electromagnetic coupled simulation for the 2.9GHz patch antenna. In order to simulate diode nonlinear behavior such as frequency doubling, the harmonic balance simulation is indispensable. However, because COMSOL does not support a harmonic balance functionality, Advanced Design System (ADS) software package is used to analyze the second harmonic wave from the output side of the Schottky diode to accomplish the matching network design. The simulation results are further verified by lab experiments.

The rest of this paper is organized as follows. Section II describes the operation mechanism of the frequency doubling antenna sensor. Section III presents the design of each component of the sensor, including the receiving and transmitting patch antennas and a matching network in-between. Section IV estimates the strain sensing performance of the frequency doubling sensor and Section V presents results from tensile experiments and emulated crack tests. Finally, the paper is summarized with a conclusion and future work.

II. Fundamentals of Frequency Doubling Antenna Sensor for Passive Wireless Strain Sensing

This section describes how the frequency doubling technology is proposed for wireless strain and crack sensing measurement. Section A presents components of the frequency doubling antenna sensor and the associated wireless interrogation method. Section B describes the strain and crack sensing mechanism.

A. Wireless interrogation scheme of a frequency doubling antenna sensor

A frequency doubling antenna sensor consists of three main components, i.e., a receiving antenna (with resonance frequency f_{R0}), a transmitting antenna (with doubled resonance frequency $2f_{R0}$), and a diode-integrated matching network between receiving and transmitting antennas. Fig. 1 illustrates the operation mechanism of a frequency doubling sensor. During operation, a wireless interrogation signal is emitted from the reader side through a transmitting reader antenna. If interrogation frequency f is in the neighborhood of f_{R0} (resonance frequency of the receiving patch antenna at sensor side), interrogation power is captured by the sensor-side receiving patch antenna and transferred to the matching network. Due to nonlinear behavior of the diode, the output signal from the diode has significant amplitude at harmonics (multiples) of the incident frequency. In this application, the second harmonic ($2f$) of the incident frequency is utilized and to be measured by the reader. The output signal at $2f$ is backscattered to the reader through sensor-side transmitting patch antenna (resonance frequency at $2f_{R0}$). Because the unwanted environmental reflections to original reader interrogation signal remains at f, it is easy for the reader to

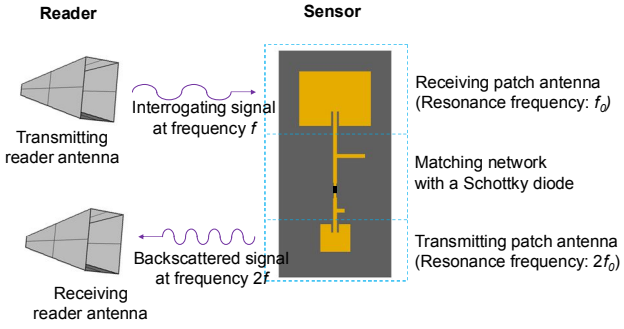

Fig. 1. Interrogation scheme of a frequency doubling antenna sensor

distinguish backscattered sensor signal from unwanted environmental reflections.

B. Strain and crack sensing using the frequency doubling antenna sensor

The frequency doubling antenna sensor can achieve wireless strain and crack sensing through detecting resonance frequency change. Once an antenna sensor is bonded on a structural surface for strain measurement, the sensor deforms together with the structure. As a result, the antenna length changes with structural deformation. Eq. (1) shows that resonance frequency of a regular patch antenna , $f_{\mathrm{R0}}^{\mathrm{Patch}}$, is related to antenna length [20]:

$$f_{\mathrm{R0}}^{\mathrm{Patch}} = \frac{c}{2(L+L')\sqrt{\beta_{\mathrm{reff}}}} \tag{1}$$

where c is the speed of the light, L is the physical length of the copper cladding on the antenna, β_{reff} is the effective dielectric constant of the antenna substrate, and L' is the additional electrical length due to fringing effect. Because the thickness-to-width ratio of a patch antenna is much smaller than one, the effective dielectric constant β_{reff} has approximately the same value as the dielectric constant β_{r0} [20] :

$$\beta_{\mathrm{reff}} = \frac{\beta_{\mathrm{r0}}+1}{2} + \frac{\beta_{\mathrm{r0}}-1}{2}\left[1+12\frac{h}{W}\right]^{-1/2} \cong \beta_{\mathrm{r0}} \tag{2}$$

where h and W are thickness and width of the substrate, respectively; β_{r0} is the relative dielectric constant of the substrate at room temperature without any deformation.

When the antenna is deformed or cracked as shown in Fig. 2(a) and (b), the length of electrical path is changed. When strain ε occurs in the longitudinal direction, the resonance frequency is shifted to:

$$f_{\mathrm{R}}^{\mathrm{Patch}} = \frac{c}{2(1+\varepsilon)(L+L')\sqrt{\beta_{r0}}} = \frac{f_{\mathrm{R0}}^{\mathrm{Patch}}}{1+\varepsilon} \tag{3}$$

If the applied strain ε is small (usually less than a few thousand microstrains), the resonance frequency of the sensor changes approximately linearly with respect to strain:

$$\begin{aligned} \mathrm{f}_R^{Patch} &= f_{\mathrm{R0}}^{\mathrm{Patch}}(1-\varepsilon+\varepsilon^2-\varepsilon^3+\varepsilon^4-\varepsilon^5+\cdots) \\ &\cong f_{\mathrm{R0}}^{\mathrm{Patch}}(1-\varepsilon) \end{aligned} \tag{4}$$

This linear relationship indicates that strain can be derived by measuring shift in the antenna resonance frequency. This serves as the fundamental strain sensing mechanism of the wireless antenna sensor. Fig. 2(a) and (b) illustrate the relationship between sensor deformation or crack development and antenna resonance frequency. When strain ε is positive, the current path is elongated. Therefore, the resonance frequency f decreases according to Eq.(4) . On the other hand, if strain ε is negative, the resonance frequency f increases (Fig. 2(c)). In addition, when a crack is propagated into the antenna sensor, the surface current is detoured and the current path also becomes longer, reducing resonance frequency. Therefore, by interrogating

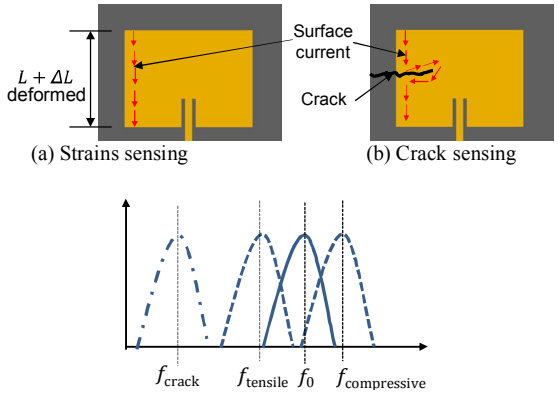

(c) Frequency change by crack and strain

Fig. 2. Strain/Crack simulation mechanism of a patch antenna sensor

frequency shift, the crack propagation can also be detected. For the frequency doubling antenna sensor, only the 2.9GHz receiving patch antenna is bonded to the structure, while other components are free from strain. When the 2.9GHz receiving patch antenna experiences strain or crack, its resonance frequency shifts from f_{R0} to $f_{\mathrm{R0}}+\Delta f$. Through the frequency doubling functionality of the match network, frequency shift of the backscattering signal changes to $2\Delta f$ correspondingly.

III. Design of the Frequency Doubling Antenna Sensor

To design the receiving patch and the transmitting patch of the antenna sensor, COMSOL radio frequency (RF) module is sufficient and thus, adopted. In order to simulate the nonlinear behavior of the frequency doubling matching network, the simulation software package should support harmonic balance simulation to characterize the second harmonic performance of the Schottky diode output, i.e. at a frequency twice the incident frequency [21]. Because the AC/DC module in COMSOL does not support harmonic balance simulation, ADS software package is adopted to design the matching network. Section A describes design of the receiving and transmitting patch antennas. Section B presents the matching network design.

A. Receiving and transmitting antenna design

The Rogers RT/duriod®5880 material is a glass micro-fiber reinforced PTFE with a low dielectric constant ($\varepsilon_r = 2.2$) and a low tangent loss (0.0009). The material is used as the antenna sensor substrate to improve interrogation distance and signal-to-noise. The thickness of the substrate is 0.7874mm (31mil). As shown in Fig. 3(a), the planar dimension of the receiving patch antenna is 44.45mm × 32.29mm, operating at the 2.9GHz frequency range. The scattering parameter S_{11} characterizes radiation efficiency of the antenna at a certain frequency level and is calculated as:

$$S_{11} = \frac{V_{\mathrm{out}}}{V_{\mathrm{in}}} \tag{5}$$

where V_{in} and V_{out} are input (incident) and output (reflected) voltage at the 50 Ohm lumped port.

If the output (reflected) voltage is small at certain frequency, most of the input energy is radiated into the air, which means

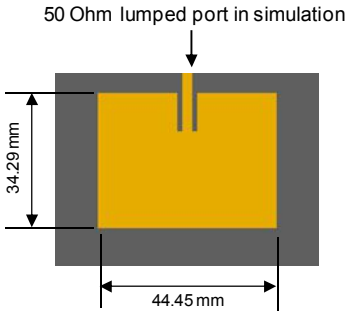

(a) Dimensions of the 2.9GHz receiving patch antenna

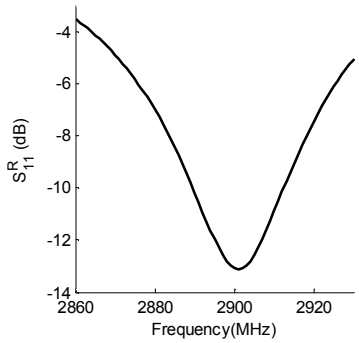

(b) Simulated S_{11}^R parameter

Fig. 3. Sensor-side receiving antenna design

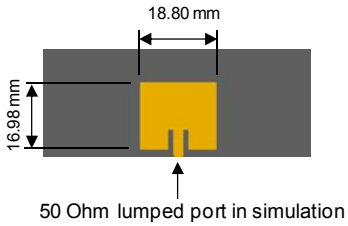

(a) Dimensions of the 5.8GHz transmitting patch antenna

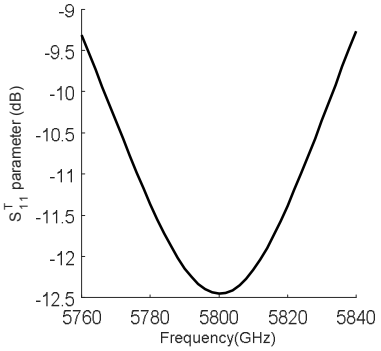

(b) Simulated S_{11}^T parameter

Fig. 4. Sensor-side transmitting patch antenna design

the antenna has high radiation efficiency at that frequency. Therefore, scattering parameter S_{11} can be utilized to decide the antenna's resonance frequency by picking the frequency corresponding to the minimum value of $|S_{11}|$. COMSOL simulation shows the scattering parameter of the receiving antenna named S_{11}^R is –13dB at 2.9GHz, as shown in Fig. 3(b). This is lower than the required –10dB return loss threshold of a typical antenna, indicating high radiation efficiency.

Designed on the same substrate, dimension of the 5.8GHz transmitting patch antenna is 18.80mm × 16.98mm (Fig. 4(a)). As shown in Fig. 4(b), the simulated scattering parameter S_{11}^T is –12.5dB at 5.8GHz which is twice the value of the receiving antenna's resonance frequency, and thus achieves frequency doubling.

B. Matching network design

The main goal of the matching network design is to maximize output power (at Port 2) upon frequency doubling (Fig. 5(a)). To this end, a stub matching technique is used between input and output of the diode, in order to match impedances between the diode and two patch antennas. The diode in the matching network, which is a two-terminal semiconductor device, offers a nonlinear relationship between excitation voltage and current. This nonlinearity produces the second harmonic wave (i.e. doubling frequency) at the output terminal. A Schottky diode is selected in this research due to its relatively low junction capacitance, allowing operation at high frequency. The overall size of the matching network is 70.00mm × 55.88mm (Fig. 5(a)). To validate the design performance, the power loss due to diode-integrated matching network is investigated by a harmonic balance simulation in a commercial circuit simulation software package, ADS. The SPICE diode model is used to simulate the performance of the Schottky diode. Conversion gain is an index to show how matching network is well designed for frequency doubling. Conversion gain in the frequency doubling process is defined as:

$$G_C = \frac{P_2}{P_1} \tag{6}$$

where P_1 is input power at frequency f to Port 1; P_2 is output power with doubled frequency $2f$ from Port 2 (Fig. 5(a)).

In ADS simulation, the input power to Port 1 (P_1) in the matching network is set to –10dBm. The value is obtained from an experimental measurement by setting the reader interrogation power at 15dBm and the reader 12 in. away from the sensor. The simulated conversion gain is plotted in Fig. 7(b). The gain is around –13 dB at the interrogation frequency band.

IV. MULTI-PHYSICS COUPLED SIMULATION FOR FREQUENCY DOUBLING ANTENNA SENSOR

A special three-step simulation is proposed in order to simulate strain sensing performance of the entire frequency doubling antenna sensor. Fig. 6 shows the flow chart of the three-step coupled simulation. The mechanical behavior of the 2.9GHz sensor-side receiving antenna under strain is first simulated in COMSOL. Electromagnetic simulation is then performed with the deformed antenna shape. The mechanical-electromagnetic coupled simulation results

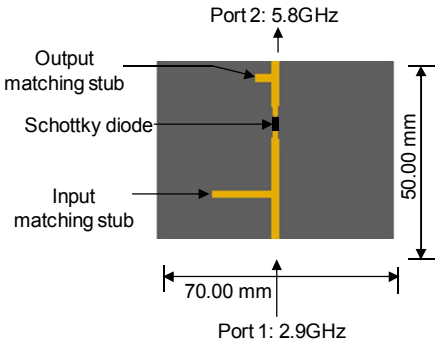

(a) Dimensions of the matching network

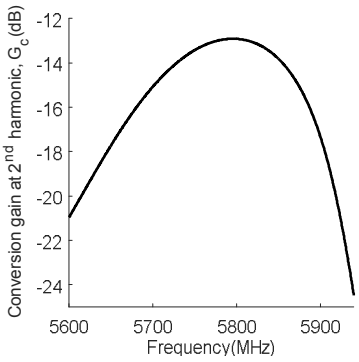

(b) Simulated conversion gain at the 2nd harmonic, G_c at -10 dBm input power

Fig. 5. Matching network design

produce power P_1 at different strain levels, which serves as input power to the matching network at Port 1. The following simulation of the diode-integrated matching network in ADS then generates the output power P_2 at the doubled frequency. With output power P_2 from ADS simulation, the 5.8GHz transmitting patch antenna finally backscatters the overall response signal of power P to the reader. Section A describes the mechanical-electromagnetic coupled simulation for the 2.9GHz receiving patch antenna at different strain levels. Section B introduces simulation setup and results for the matching network design. Section C presents backscattered signal from the 5.8GHz transmitting antenna.

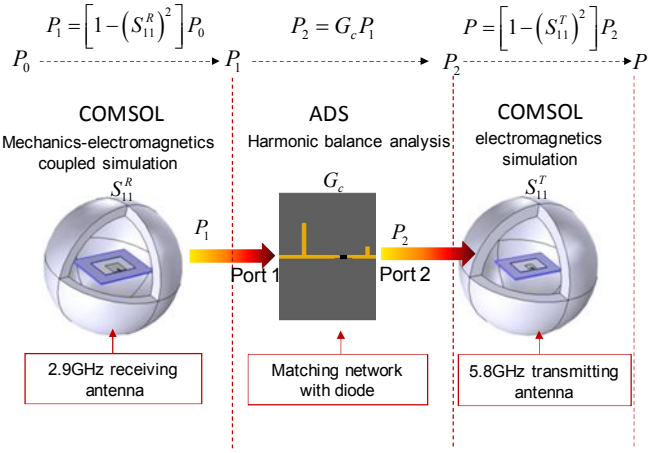

Fig. 6. Flow chart of the multi-physics coupled simulation for the entire sensor

A. The mechanical-electromagnetic coupled simulation of 2.9GHz patch antenna

In this preliminary study, it is proposed that only the 2.9GHz receiving patch antenna is bonded on the structural surface, while other parts of the sensor (the matching network and the 5.8GHz patch antenna) are not. Therefore, the 2.9GHz sensor-side receiving antenna not only receives interrogation power from the reader, but also serves as the strain sensing element. While the 2.9GHz antenna experiences strain with structural surface, all other parts of the sensor are strain free. Therefore, a mechanical-electromagnetic coupled simulation is required for the 2.9GHz patch antenna model, in order to accurately describe the electromagnetic performance of the patch antenna under strain.

Fig. 7(a) shows the COMSOL mechanical-electromagnetic coupled simulation model of the 2.9GHz patch antenna. The 2.9GHz patch antenna, together with an aluminum plate, is placed in the center of an air sphere. Outside of the air sphere is the PML (perfectly matched layer), which is used to truncate the simulation domain to be finite. Key material properties of the simulation model are described in Table 1. Different element types of the finite element model are adopted to better simulate the antenna structure. Table 2 lists the number of each type of the element, and the corresponding DOFs in COMSOL model.

To investigate the strain sensing capability of the sensor, prescribed displacements are applied to the two ends of the aluminum plate. Five strain levels are applied from zero to 2,000με, with 500με strain change per step. Fig. 7(b) shows S_{11} plot of the 2.9GHz patch antenna under different strain levels. The resonance frequency of the antenna at zero strain level is

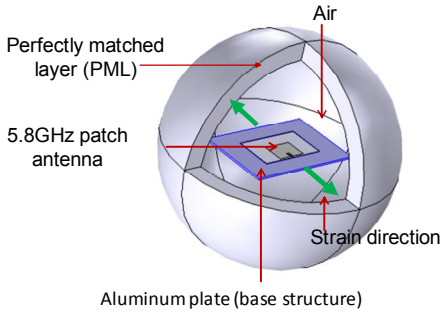

(a) Multi-physics simulation model of the 2.9 GHz receiving antenna

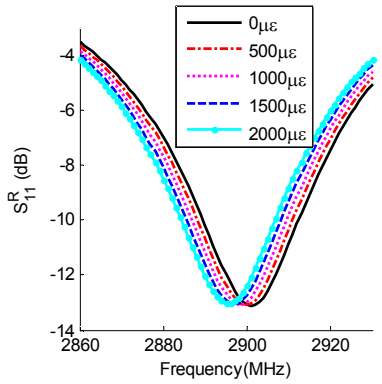

(b) Simulated S_{11}^R parameter under strain

Fig. 7. Multi-physics modeling and simulation for the receiving (2.9 GHz) patch antenna

Table 1. Key material properties of the receiving 2.9GHz patch antenna

	Substrate	Copper cladding	Aluminum
Material type	Glass microfiber reinforced PTFE	Copper	6061 Aluminum alloy
Relative permittivity (β_{reff})	2.2	-	-
Conductivity (S/m)	0.5×10^{-9}	PEC	PEC
Young's modulus (GPa)	1.07	110	69

Table 2. Number of elements and degrees of freedom in the 2.9GHz patch antenna model

Number of elements		Number of DOFs	
Tetrahedron	39,665	Mechanics	53,124
Prism	3,220		
Triangle	5,768	Electromagnetics	477,429

around 2.901GHz, which is the same as shown in Fig. 3(b). As the applied strain increases, the antenna resonance frequency decreases gradually, as expected.

B. The harmonic balance simulation of the matching network

The power flow through the 2.9GHz receiving patch antenna to the input port (Port 1) of the matching network is described as:

$$P_1 = [1 - (S_{11}^{R})^2]P_0 \quad (7)$$

where P_0 is set to –10dBm from experimental measurement and S_{11}^{R} from different strain levels are obtained by COMSOL simulation, as presented in Fig. 7(b).

To characterize backscattering resonance of the sensor, sensor response for a neighborhood frequency range needs to be analyzed. With P_1 as input, conversion gain G_C of the matching network, generated by the harmonic balance simulation in ADS, is used to calculate the output power at Port 2 of the matching network as $P_2 = G_C P_1$. The output power result is plotted in Fig. 8. For example, at zero strain level, the frequency at the peak of P_2 is around 5.750GHz. While at

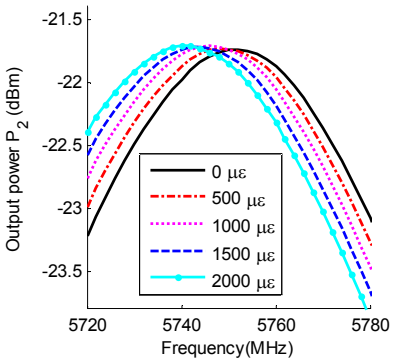

Fig. 8 Output power P_2 from matching network

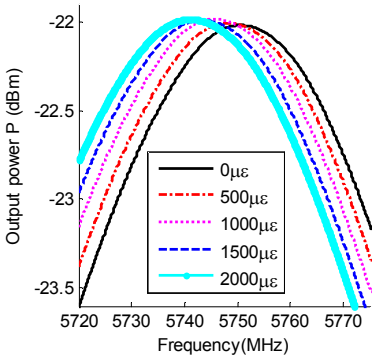

(a) Output power with different strain level

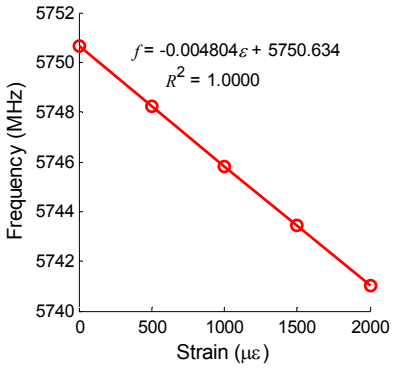

(b) Resonance frequency versus strain curve

Fig. 9. Multi-physics simulation result

1,000με, the peak frequency reduces to around 5.745GHz.

C. Backscattered signal at the 5.8GHz antenna

The final step of the sensor operation is to let the power P_2 flow through the 5.8GHz patch antenna. The simulated scattering parameter S_{11}^{T} is needed to estimate overall output power P:

$$P = [1 - (S_{11}^{T})^2]P_2 \quad (8)$$

The simulation results for overall output power P are shown in Fig. 9(a). Resonance frequency of the entire sensor decreases as applied strain increases. The resonance frequency at each strain level is extracted from Fig. 9(a), and linear regression is performed to plot the relationship between strain and resonance frequency in Fig. 9(b). The figure shows a strain sensitivity of –4.804 kHz/με, which is more than five times higher than the RFID-based antenna sensor [17]. In addition, the coefficient of determination is close to be one, which indicates a good linearity.

V. Experimental Validation

In order to validate the sensor performance, two experimental tests were conducted. Strain sensing performance is described in Section A. Emulated crack sensing performance is described in Section B

A. *Strain sensing experiments*

The photo of a fabricated frequency doubling sensor is shown Fig. 10. The planar dimension of the frequency doubling antenna sensor is 140mm × 70mm. To improve the energy transmission efficiency across the matching network, a 33nH inductor is installed in parallel with the Schottky diode.

During the strain sensing test, only the 2.9GHz transmitting antenna is bonded to the surface of an aluminum plate (similar to the plates used in [17, 18]), while all other components float over the structural surface. Following the setup in Fig. 1, the interrogation distance between reader antennas and the sensor is set as 504mm (20in.). The tensile loading to the aluminum plate is increased to generate strain up to 300με with 50με increment per loading step. The received power at different frequencies are recorded. For clarity, only four strain levels are plotted in Fig. 11(a). The resonance frequencies at different strain levels are thus extracted and plotted in Fig. 11(b), showing a strain sensitivity of −5.232kHz/με and a determination coefficient of 0.9890.

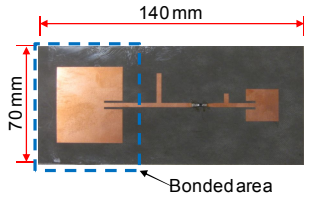

Fig. 10. Photo of the fabricated sensor

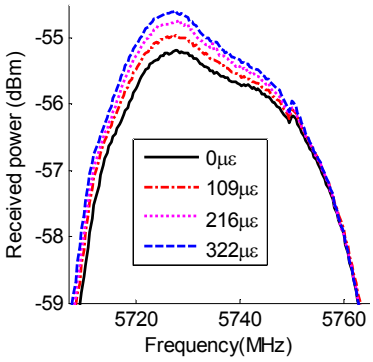

(a) Average received power

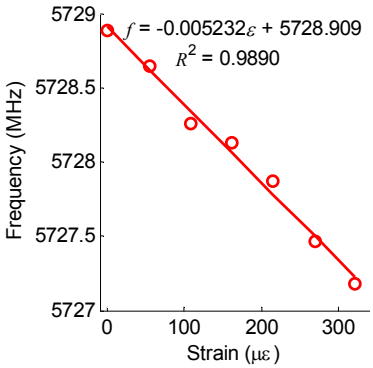

(b) Resonance frequency change versus strain

Fig. 11. Tensile test results of frequency doubling antenna sensor

B. *Emulated crack sensing*

In order to conveniently generate crack propagation into the sensor, an emulated crack device is designed and fabricated as shown in Fig. 12. The crack testing device consists of three aluminum plates, i.e. a base plate, a rotating top plate, and a fixed bottom plate. Because the three plates are relatively thick, the plates can be assumed to be rigid. The fixed bottom plate is fastened to the base plate by four corner bolts. The rotating top plate is attached to the base plate by one bolt at the bottom right corner, which acts as the rotation axis. By rotating a control screw, the rotation of the top plate opens a crack/gap between the top and bottom plates. The 2.9GHz receiving patch antenna of the frequency doubling sensor is installed on the crack opening line (dashed line in Fig. 12), between the fixed and rotating plates. The crack opening size is measured by a digital dial gage (2.54μm resolution) mounted at the left side of the base plate.

During wireless interrogation, the interrogation distance between reader antennas and the sensor is 508mm (20inches). The crack size opens from zero to 4.47mm (176mils) in a total number of 23 steps. Crack size underneath the sensor is estimated from dial gage reading. Fig. 13 shows representative photos of the deformed/cracked antenna sensor at three example crack opening sizes. Fig. 13(a) shows the sensor at 18-mil crack opening. No fracture occurs on the sensor, but slight deformation is observed on the top copper cladding. Fig. 13(b) shows when crack opening is 1,160μm (40mils), small fractures have developed on the top copper and the substrate, but the sensor still functions properly.

The loading step after 216mils causes rapid breakage of the sensor, as shown in Fig. 13(c). At this point, the crack grows through the entire antenna width. No response from the antenna sensor can be received by the reader. For clarity, Fig. 14(a) and (b) each shows the received power plots for only five crack opening sizes. The resonance frequency shift is easily observable in both plots. Upon extracting resonance frequency at each crack growth level from the received power plot, Fig. 15(a) shows resonance frequency change as crack size increases, while Fig. 15(b) zooms in to the area with crack size less than 0.76mm (30mils). A monotonic decrease in the resonance frequency is observed when the crack width increases. When the crack fully propagates through the patch

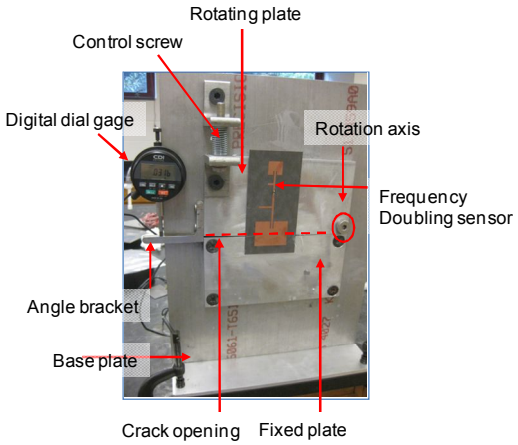

Fig. 12 Emulated crack device

(a) Crack width 460 μm (18 mils)

(b) Crack width 1,160 μm (40 mils)

(c) Crack width 5,490 μm (216 mils)

Fig. 13. Photos of deformed antenna sensor at different crack opening sizes

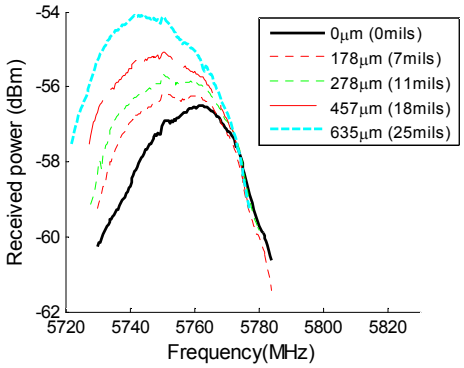

(a) Crack size from 0 to 25mils

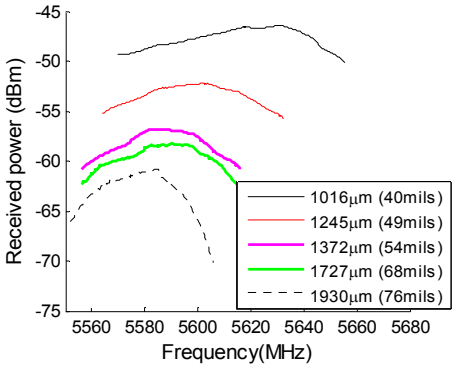

(b) Crack size from 40 to 76 mils

Fig. 14 Emulated crack device

antenna, the largest observed frequency shift is 160MHz.

VI. Summary and Discussion

In this research, a novel frequency doubling technique is proposed for a passive (batter-free) wireless strain/crack measurement. A 2.9 to 5.8GHz frequency doubling antenna sensor is designed. The wireless strain sensing performance is estimated by multi-physics modeling and simulation. Validation experiments are conducted to characterize wireless strain/crack sensing performance. Tensile testing shows a strain sensitivity of −5.232kHz/με and a determination coefficient of 0.9890. The strain sensitivity of the frequency doubling sensor is around five times of previously developed RFID antenna sensors. In addition, a large amount of resonance frequency shift of the frequency doubling antenna sensor is observed in

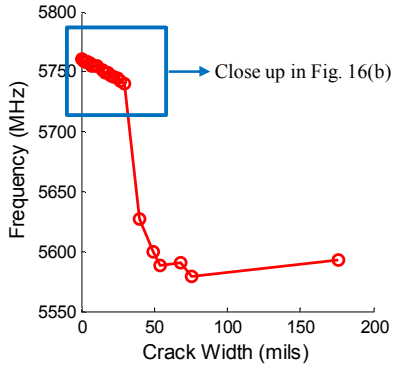

(a) Resonance frequency change during crack growth

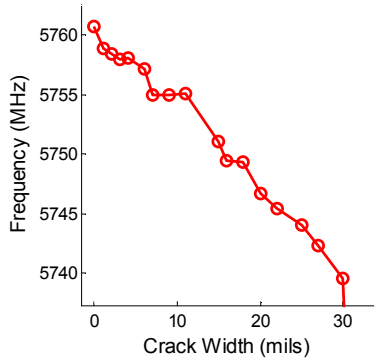

(b) Resonance frequency change during crack growth (closed-up view to 0-30mils)

Fig. 15. Resonance frequency change during crack growth

the emulated crack test [17]. The experimental results demonstrate the potential of the frequency doubling antenna sensor for both strain and crack sensing.

Future research is needed to improve the reliability of the antenna sensor, particularly for different reader-sensor distances and interrogation power levels. In order to maximize the sensing performance, more systematic approach is required to optimize the frequency doubling antenna sensor design. Finally, a mechanism for signal collision avoidance is under development, in order to allow multiple sensors to operate in the close proximity.

References

[1] H. Sohn, C. R. Farrar, F. M. Hemez, D. D. Shunk, D. W. Stinemates, and B. R. Nadler, "A Review of Structural Health Monitoring Literature: 1996-2001," Los Alamos National Laboratory, Los Alamos, NM Report No. LA-13976-MS, 2003.

[2] M. Çelebi, "Seismic Instrumentation of Buildings (with Emphasis on Federal Buildings)," United States Geological Survey, Menlo Park, CA Report No. 0-7460-68170, 2002.

[3] E. G. Straser and A. S. Kiremidjian, "A Modular, Wireless Damage Monitoring System for Structures," John A. Blume Earthquake Eng. Ctr., Stanford University, Stanford, CA Report No. 128, 1998.

[4] J. P. Lynch, K. H. Law, A. S. Kiremidjian, C. E., C. R. Farrar, H. Sohn, *et al.*, "Design and performance

validation of a wireless sensing unit for structural health monitoring applications," *Structural Engineering and Mechanics,* vol. 17, pp. 393-408, 2004.

[5] Y. Wang, J. P. Lynch, and K. H. Law, "A wireless structural health monitoring system with multithreaded sensing devices: design and validation," *Structure and Infrastructure Engineering,* vol. 3, pp. 103-120, 2007.

[6] J. P. Lynch and K. J. Loh, "A summary review of wireless sensors and sensor networks for structural health monitoring," *The Shock and Vibration Digest,* vol. 38, pp. 91-128, 2006.

[7] G. Park, T. Rosing, M. D. Todd, C. R. Farrar, and W. Hodgkiss, "Energy harvesting for structural health monitoring sensor networks," *Journal of Infrastructure Systems,* vol. 14, pp. 64-79, March 2008 2008.

[8] A. Deivasigamani, A. Daliri, C. H. Wang, and S. John, "A review of passive wireless sensors for structural health monitoring," *Modern Applied Science,* vol. 7, pp. 57-76, 2013.

[9] J. C. Butler, A. J. Vigliotti, F. W. Verdi, and S. M. Walsh, "Wireless, passive, resonant-circuit, inductively coupled, inductive strain sensor," *Sensors and Actuators A: Physical,* vol. 102, pp. 61-66, 2002.

[10] K. J. Loh, J. P. Lynch, and N. A. Kotov, "Inductively coupled nanocomposite wireless strain and pH sensors," *Smart Structures and Systems,* vol. 4, pp. 531-548, 2008.

[11] Y. Jia, K. Sun, F. J. Agosto, and M. T. Quinones, "Design and characterization of a passive wireless strain sensor," *Measurement Science and Technology,* vol. 17, pp. 2869-2876, Nov 2006.

[12] R. Matsuzaki, M. Melnykowycz, and A. Todoroki, "Antenna/sensor multifunctional composites for the wireless detection of damage," *Composites Science and Technology,* vol. 69, pp. 2507-2513, 2009.

[13] A. Daliri, A. Galehdar, S. John, C. H. Wang, W. S. T. Towe, and K. Ghorbani, "Wireless strain measurement using circular microstrip patch antennas," *Sensors and Actuators A: Physical,* vol. 184, pp. 86-92, 2012.

[14] R. Melik, N. K. Pergoz, E. Unal, C. Puttlitz, and H. V. Demir, "Bio implantable passive on-chip RF-MEMS strain sensing resonators for orthopedic application," *Journal of Micromechanics and Microengineering,* vol. 18, p. 115017, 2008.

[15] S. Deshmukh and H. Huang, "Wireless interrogation of passive antenna sensors," *Measurement Science and Technology,* vol. 21, 2010.

[16] X. Xu and H. Huang, "Battery-less wireless interrogation of microstrip patch antenna for strain sensing," *Smart Materials and Structures,* vol. 21, p. 125007, 2012.

[17] X. Yi, C. Cho, J. Cooper, Y. Wang, M. M. Tentzeris, and R. T. Leon, "Passive wireless antenna sensor for strain and crack sensing-electromagnetic modeling, simulation, and testing," *Smart Materials and Structures,* vol. 22, p. 085009, 2013.

[18] X. Yi, T. Wu, Y. Wang, R. T. Leon, M. M. Tentzeris, and G. Lantz, "Passive wireless smart-skin sensor using RFID-based folded patch antennas," *International Journal of Smart and Nano Materials,* vol. 2, pp. 22-38, Jan 2011.

[19] EPCglobal Inc., "EPC^{TM} Radio-frequency Identity Protocols Class-1 Generation-2 UHF RFID Protocol for Communications at 860 MHz-960 MHz " EPCglobal Inc. Version 1.2.0, 2008.

[20] C. A. Balanis, *Advanced Engineering Electromagnetics*. New York: Wiley & Sons, 1989.

[21] S. A. Maas, *Nonlinear Microwave and RF Circuits*, 2nd ed. Norwood, MA: Artech House, 2003.